

Supporting information

Wearable wire-shaped symmetric supercapacitors based on activated carbon coated graphite fiber

*Chan Wang,^{†,‡,¶} Kuan Hu,^{†,‡,¶} Wenjian Li,^{†,‡} Huaying Wang,^{†,‡} Hu Li,^{†,‡,§} Yang Zou,^{†,‡}
Chaochao Zhao,^{†,‡} Zhe Li,^{†,‡} Min Yu,^{†,‡} Puchuan Tan,^{†,‡} Zhou Li^{*,†,‡,¶}*

[†]CAS Center for Excellence in Nanoscience, Beijing Key Laboratory of Micro-nano Energy and Sensor, Beijing Institute of Nanoenergy and Nanosystems, Chinese Academy of Sciences, Beijing 100083, P. R. China; [‡]School of Nanoscience and Technology, University of Chinese Academy of Sciences, Beijing 100049, P. R. China; [¶]Center on Nanoenergy Research, School of Physical Science and Technology, Guangxi University, Nanning, 530004, P. R. China; [§]Key Laboratory for Biomechanics and Mechanobiology of Ministry of Education, School of Biological Science and Medical Engineering, Beihang University, Beijing 100083, P. R. China. [¶]These authors contributed equally to this work.

Corresponding Author: Zhou Li

* Address correspondence to zli@binn.cas.cn

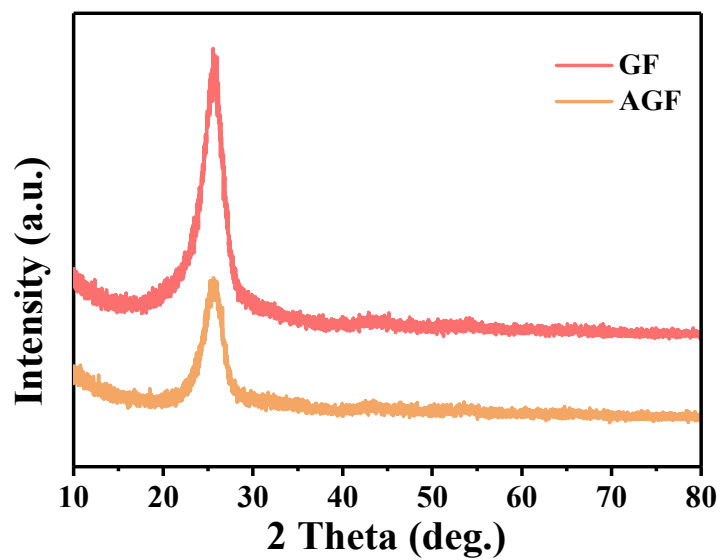


Figure S1. The XRD spectras of GF and AGF.

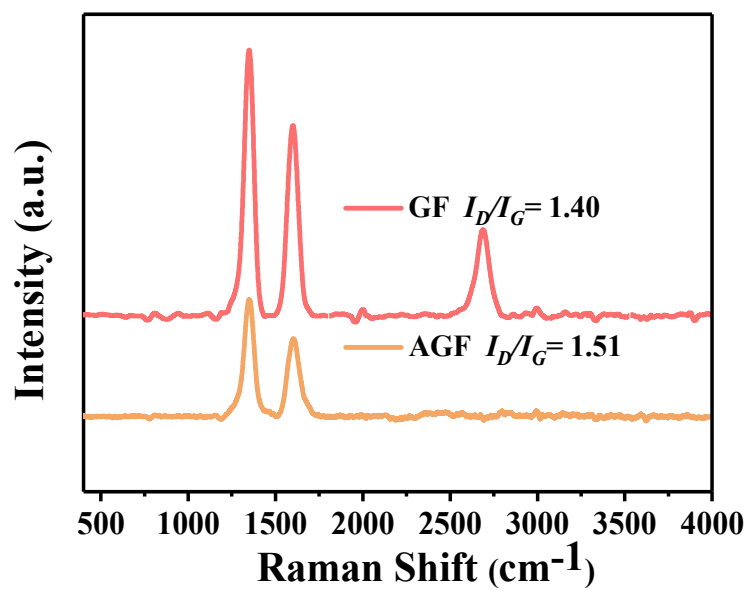


Figure S2. The Raman spectras of GF and AGF. The I_D/I_G of GF and AGF was 1.4 and 1.51, respectively.

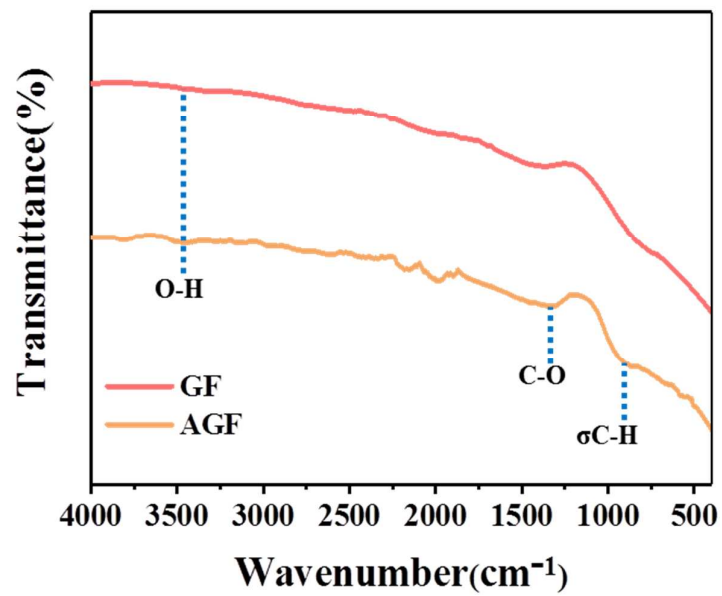


Figure S3. FTIR spectras of GF and AGF.

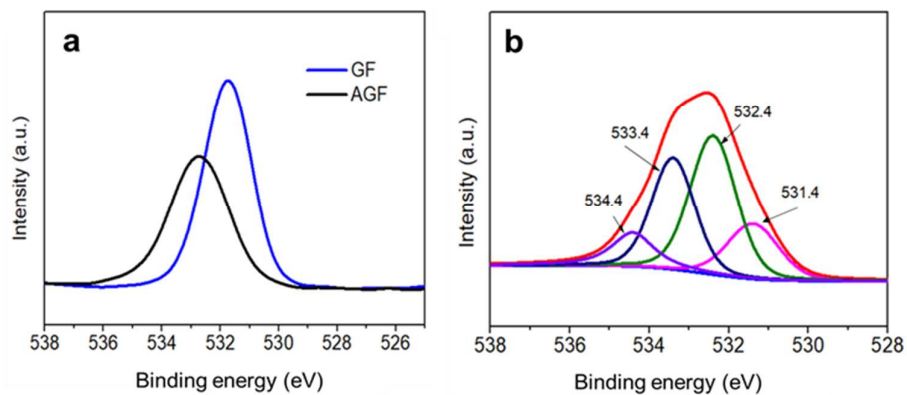


Figure S4. XPS spectra about O1s of GF (a) and AGF (b).

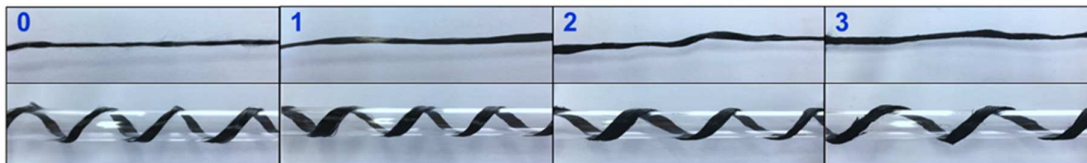


Figure S5. Optical photograph of composite electrodes of none coating (0), coating one time (1), two times (2) and three times (3).

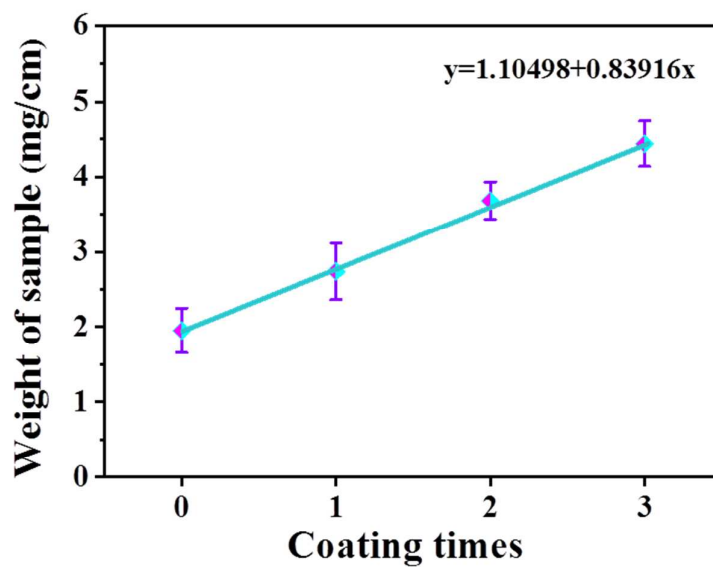


Figure S6. The relationship between the amount of AC and the number of coating times satisfies the equation $y=1.10498 + 0.83916*x$, where x refers to the coating time.

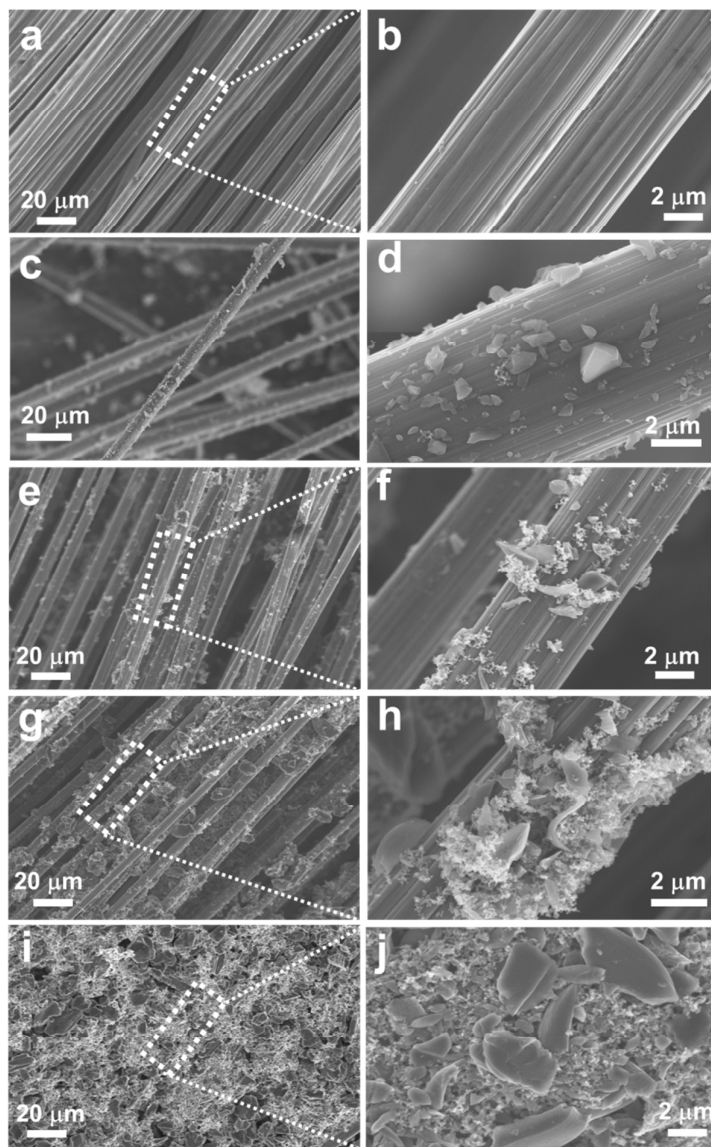


Figure S7. Morphology of the graphite fiber coated with activated carbon. (c, d) Graphite fiber without activation coated with activated carbon one time; SEM images of the activated graphite fiber coated with activated carbon by different coating times: (a, b) none coating, (e, f) coating one time; (g, h) two times; (i, j) three times. Scale bars, 20 μm (a, c, e, g, i), 2 μm (b, d, f, h, j).

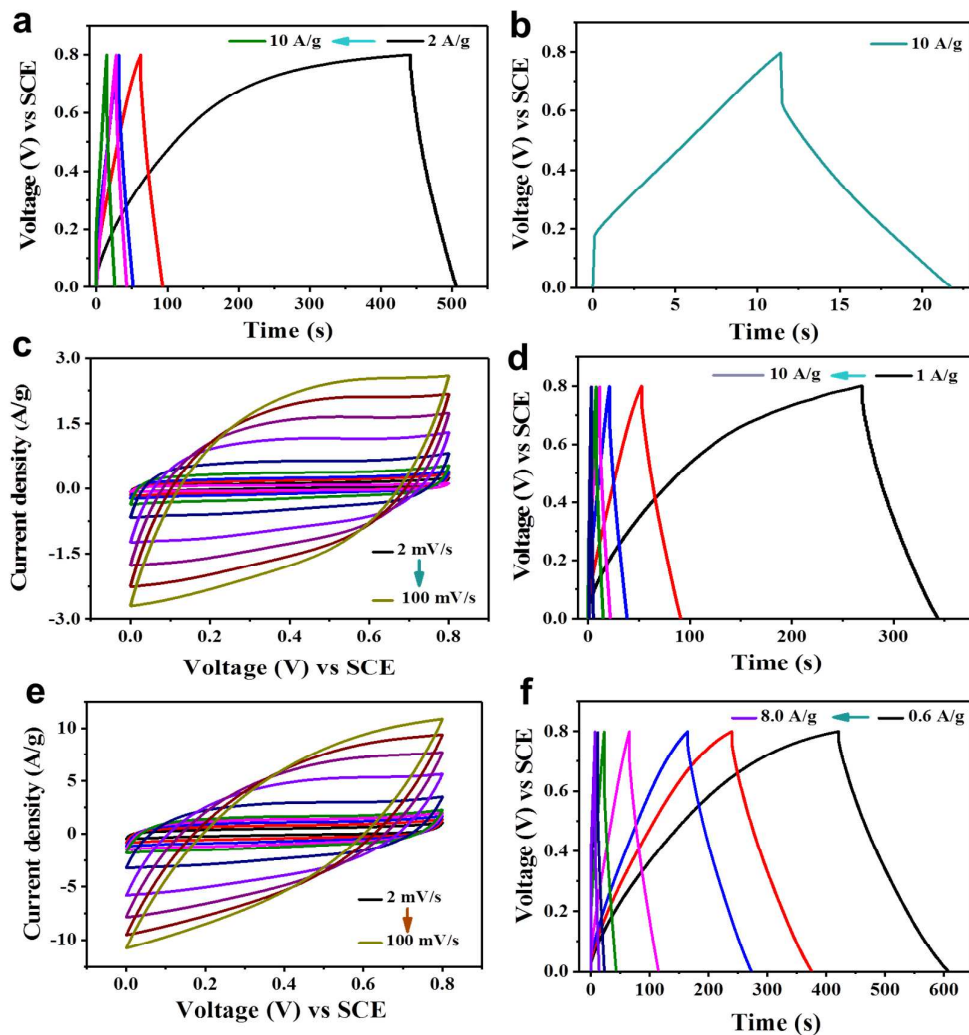


Figure S8. Electrochemical performance of composite electrodes. (a) GCD curves of AGF@AC-1 at current densities from 2-10 A/g. (b) GCD curve of the AGF@AC-1 fiber electrode at the high current density of 10 A/g. CV and GCD (c, d) curves of AGF@AC-2 at different scan rates and different current densities. CV and GCD curves (e, f) of AGF@AC-3 at different scan rates and different current densities. All above test were performed with 1.0 M aqueous H_2SO_4 electrolyte in the three-electrode cell using AGF@AC as working electrode.

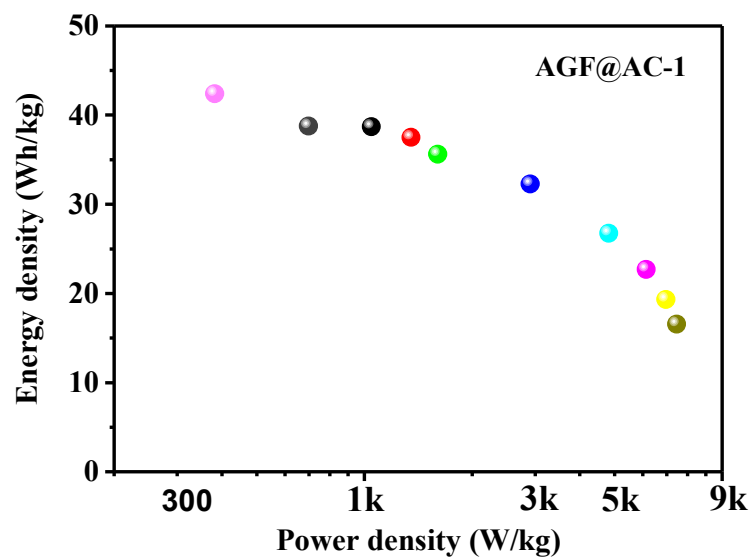


Figure S9. Ragone plot with energy density and power density calculated from AGF@AC-1 electrode.

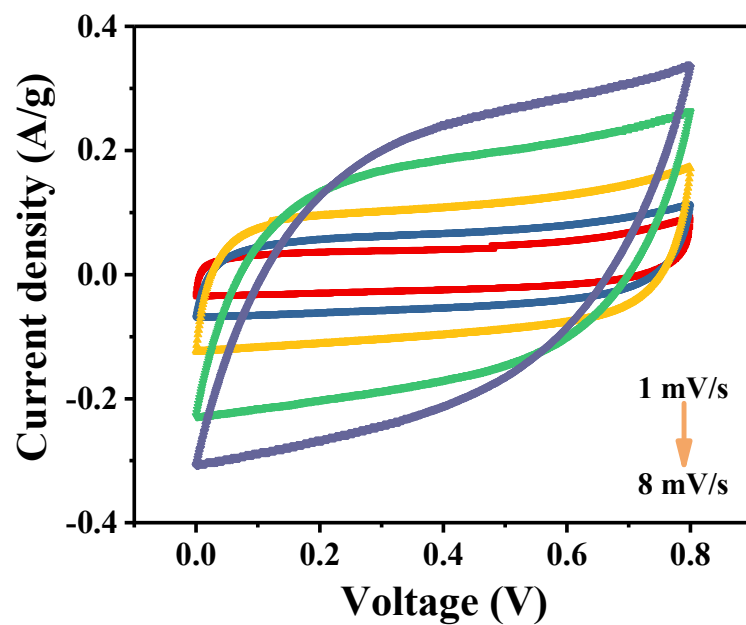


Figure S10. The CV curves of wire-shaped SC at scan rates from 1 to 8 mV/s.

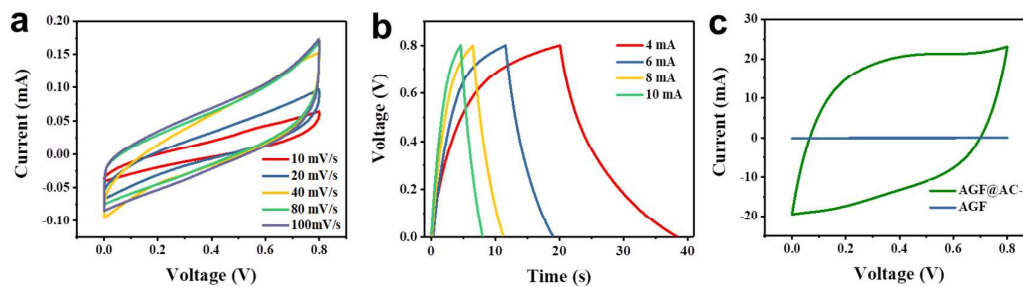


Figure S11. Electrochemical performance of all-solid-state supercapacitor based on AGF and the comparison between the SC and PWSC. (a) CV curves of all-solid-state supercapacitor based on AGF at different scan rate from 10-100 mV/s. (b) GCD curves of all-solid-state supercapacitor based on AGF at different current from 6 mA to 10 mA. (c) GCD curve of the all-solid-state supercapacitor based on AGF/AGF@AC-1 at a scan rate of 40 mV/s.

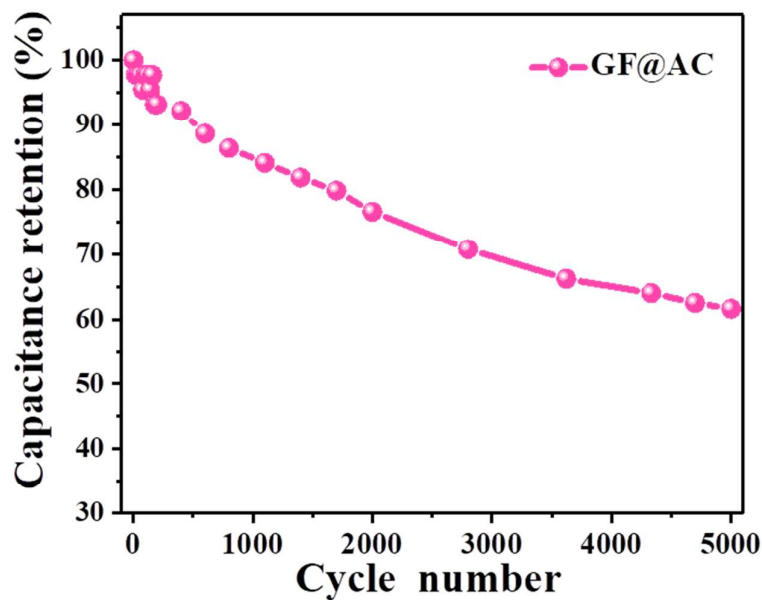


Figure S12. Cycle stability of wire-shaped SCs based on GF@AC at a current density of 2 A/g.

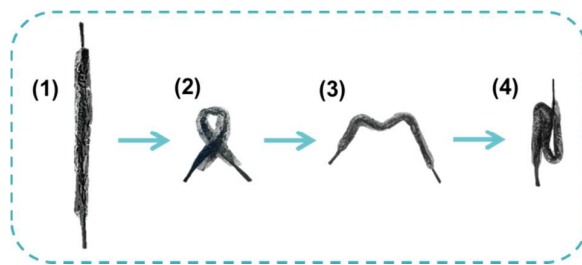


Figure S13. The optical photograph of the SC in shape of straight (1), red cross (2), M symbol (3), N symbol (4).

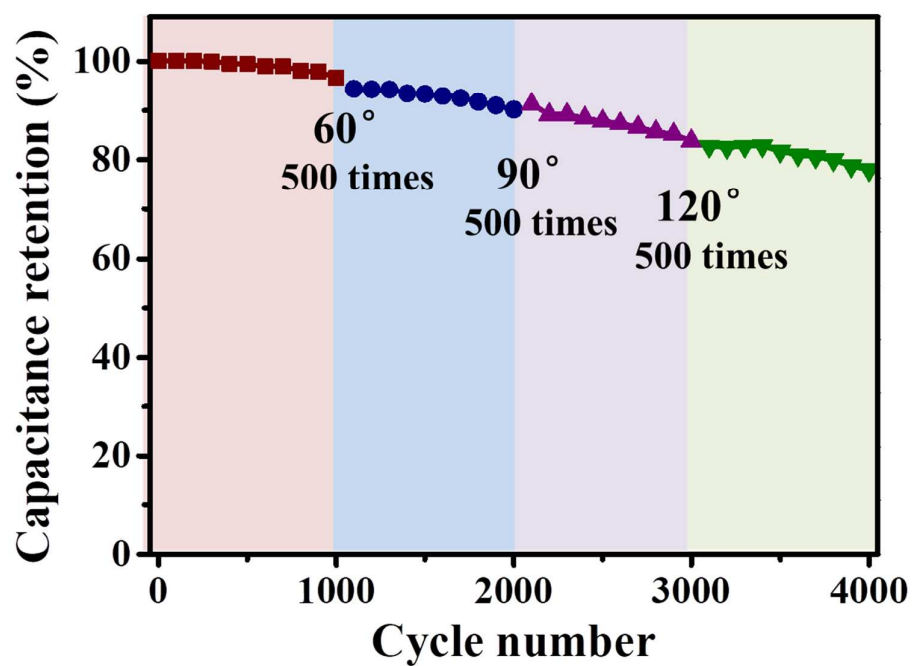


Figure S14. Cyclic charging and discharging test of wire-shaped SCs after bending into different angles (0° , 60° , 90° , 120°) in sequence.

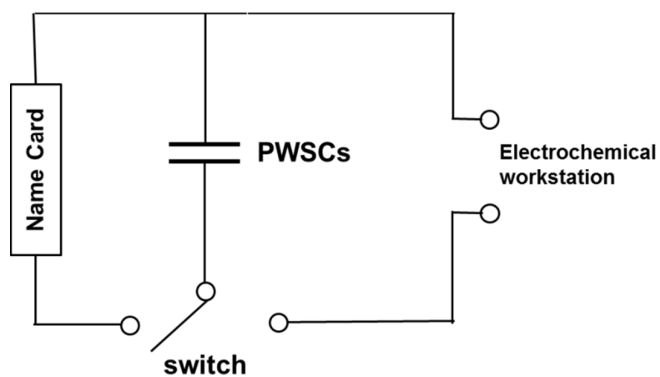


Figure S15. The logical circuit of the system consisted of name card and PWSCs. Electrochemical workstation was used to charging PWSCs. The switch was used to guide circuit. The unit of PWSCs, which was consisted of three groups connected in parallel and each group was made up of four SCs linked in series. This logical circuit was also used in supplementary video named Movie 1.

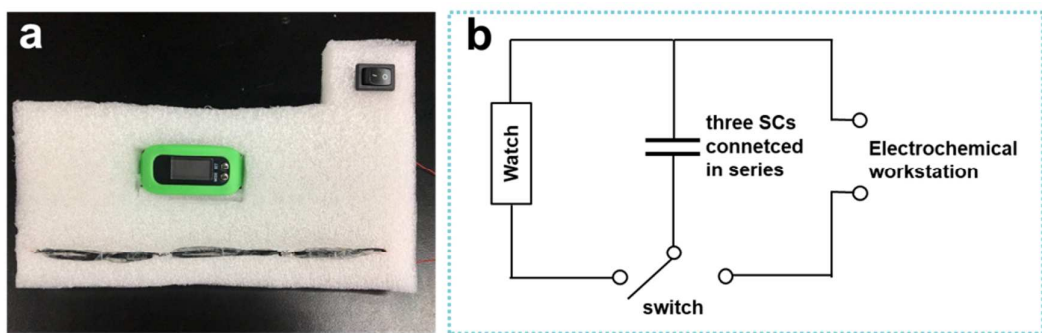


Figure S16. (a) The optical photograph of circuit consisted of three SCs connected in series, watch, and switch. (b) The logical circuit of the system in (a). (a) and (b) were used in supplementary video named Movie 2.

Table S1. The specific value of energy density and power density calculated by CV at different scan rates used in Figure S8.

Scan rate (mV/s)	2	4	6	8	10	20	40	60	80	100
Energy density (wh/kg)	42.40	38.78	38.72	37.51	35.63	32.29	26.76	22.70	19.33	16.56
Power density (kW/kg)	0.38	0.70	1.05	1.35	1.60	2.91	4.82	6.13	6.96	7.45

Table S2. The comparison about the electrochemical performance of all-solid-state supercapacitor in this work and others.

Materials	Specific capacitance	Energy intensity	Power intensity	Reference
AC/AGF	66 F/g, 81 mF/cm	6.596 Wh/kg, 8.08 mWh/cm	253 mW/kg, 0.31 mW/cm	This work
MWCNTs/CMF	5.1 mF/cm	0.7 μ Wh/cm	13.7 μ W/cm	[23]
PANI/HCNFs	339.3 F/g, 85.1 mF/cm	11.6 Wh/kg, 3.0 mWh/cm	24.5 W/kg, 6.3 mW/cm	[11]
Ppy/MnO ₂ /rGO	31 mF/cm	1.4 mWh/cm	1.3 mW/cm	[48]
Graphene sheet	185 F/g, 4.63 mF/cm	15.5 Wh/kg	4.3 mW/kg	[28]
CuHCF@CFs and PC@CFs	19.2 F/g	10.6 Wh/kg, 10.3 mWh/cm	50.6 W/kg, 49.17 mW/cm	[49]
AGF	0.29 mF/cm	0.68 mWh/cm ³	3.3 W/cm ³	[33]
rGO/AC fiber	43.8 F/g	3.96 mWh/kg	7.92 mW/kg	[39]